

## Dependence of the Cell Resistance on External Potential in DMFC System

by

Noriko OIKAWA<sup>\*</sup>, Lorene L. ABELLA<sup>\*\*</sup>, Satoshi FUKADA<sup>\*\*\*</sup>, Tatsuya MATSUMOTO<sup>†</sup>

and Kenji FUKUDA<sup>††</sup>

(Received August 18, 2011)

### Abstract

The polarization properties of a portable direct methanol fuel cell (DMFC) subjected to an external potential are experimentally investigated. In DMFC, polymer electrolyte membrane plays important role as a proton conductor. The resistance of the membrane, which reflects ion-transport and mobility of ions through the membrane, is one of the fundamental factors that determine electric activity of the fuel cell. We applied an external potential in the reverse and forward direction to the cell potential of the DMFC system. From the dependencies of the effective membrane resistance on the external potential, it was found that there are several thresholds in the external potential at which the main reactions of the cell are switched. In the case of the reverse external potential, electrolysis of water and methanol induced by the accumulated electrons and protons reduce the cell resistance. For the forward external potential, on the other hand, the resistance becomes high due to the polarization inside the membrane. The resistance decreases as electric decomposition of water and methanol proceeds.

**Keywords:** DMFC, Fuel cell system, External potential, Water electrolysis, Methanol electrolysis, Cell resistance, Cell voltage, Cell current, Methanol concentration, Electric decomposition

### 1. Introduction

Most of fuel cells are powered by hydrogen, which is mainly generated by reforming hydrogen-rich fuels such as methanol, ethanol, and hydrocarbons. In direct methanol fuel cell (DMFC), on the other hand, liquid methanol is used as the fuel. This feature brings several

---

<sup>\*</sup> Max Planck Institute for Dynamics and Self-Organization, Germany

<sup>\*\*</sup> Mitsubishi Industries, LTD.

<sup>\*\*\*</sup> Professor, Faculty of Engineering Sciences, Department of Energy Engineering Science

<sup>†</sup> Assistant Professor, Department of Applied Quantum Physics and Nuclear Engineering

<sup>††</sup> Professor, Department of Applied Quantum Physics and Nuclear Engineering

advantages to use of DMFC. No large-scale device is needed to heat and pressurize hydrogen, and potential hazard of using hydrogen gas is avoided. Liquid methanol has a higher energy density than the gas form of hydrogen<sup>1,2)</sup>. Due to these merits DMFC is desired to be one of the main energy systems in the next generation. The DMFC system has been intensively investigated to be utilized as a commercial power source in portable electric devices<sup>3,4,5)</sup>.

In DMFC technology, however, some issues need to be solved. Firstly, since oxidation reaction of liquid methanol includes intermediate steps, which impose additional potential energy for the oxidation reaction at the anode side, efficiency of the cell reaction in liquid methanol is not sufficiently high for the commercial use. A new kind or a new composition of catalyst may be necessary to be found in order to effectively activate the oxidation reaction<sup>6)</sup>. Secondly, methanol crossover occurs through the membrane. It leads to less conversion efficiency of the electrodes. Relation between the methanol concentration and the permeability of methanol has been investigated for different kinds of membrane<sup>7,8,9,10)</sup>. Thirdly, the cell performance decreases for long time operation due to structural change of the membrane<sup>11,12)</sup>.

The schematic image of a typical DMFC system is shown in **Fig. 1**. In the anode side, methanol is electro-oxidized to CO<sub>2</sub> by the reaction,



In the cathode side, on the other hand, oxygen is reduced to water by the reaction,



Electrochemical reactions at the both electrodes proceed with the supply of gas and with the supply and extraction of electrons. A polymer electrolyte membrane which separates two electrodes works as a proton conductor. The ion transport property of the membrane is one of the factors which determine the cell activity. In order to improve the performance of the cell, therefore, it is necessary to understand the properties of the ion transport in the membrane. In general, response to an external electric field brings detailed information about the ion transfer in the system. In DMFC system the responses in cell voltage and cell current to the external electric potential reflect electric conductivity and resistance of the membrane. Especially the cell current is defined by the electrochemical properties of the cell, such as diffusivity of protons, effective potential for the electrochemical reactions and reaction rates. By applying a reverse potential, on the other hand, protons are generated through electrolysis of water and methanol at anode side. Therefore, the reverse potential has been also utilized as a hydrogen pump for a quick startup at low temperature for DMFC system<sup>13)</sup>.

In this paper polarization properties of the DMFC system are investigated with applying an external potential in the reverse and the forward direction to the original cell potential. From non-monotonous responses of the cell resistance to the external potential, it was clarified that the main reactions are switched as the external potential increases. The cell resistance becomes high when the polarization occurs and is reduced when the additional reactions, such as electrolysis of water and methanol, take place.

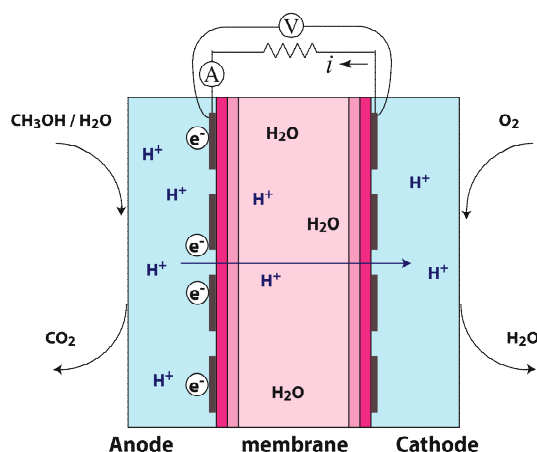


**Fig. 1** A schematic image of the DMFC system. In anode side methanol is electro-oxidized to  $\text{CO}_2$ , and in cathode side oxygen is reduced to water. Protons conduct through the polymer electrolyte membrane which separates two electrodes. The electrons are carried through the outer circuit.

## 2. Experimental

The fuel cell system used in the present experiment is described here. The outside of the anode electrode was filled with stagnant liquid methanol. In the cathode side air was supplied as a reactant gas at a constant flow rate of 80 mL/min. The cell encloses a membrane-electrode-assembly (MEA) sandwiched by two stainless-steel meshes which were used as collectors of the electricity. We used a MEA provided by Fuel Cell Store company. It consists of Nafion 117 membrane whose thickness is 180  $\mu\text{m}$  and electrodes with active area of  $2.3 \text{ cm} \times 2.3 \text{ cm}$ . The catalyst loaded on the electrodes is 4.0  $\text{mg}/\text{cm}^2$  of Pt-Ru for the anode and 2.0  $\text{mg}/\text{cm}^2$  of Pt for the cathode.

The electric circuit is schematically shown in **Fig. 2**. It should be noted that anode and cathode in fuel cell system correspond negative electrode and positive one in polarity of voltage, respectively. We used a function generator (WE7121, Yokogawa electric corporation) to generate DC signal and an isolated digitizer (WE7275, Yokogawa electric corporation) to measure the voltage and the current. DC voltage is applied to the cell through the wires attached on the each stainless steel mesh. The isolated digitizer was placed in series with the cell to measure the cell potential. The temperature was controlled by a commercial regulator (TJA-550K, AS ONE corporation). The temperature was controlled within  $18.0 \pm 0.1 \text{ }^\circ\text{C}$  through the experiments except for the case that the temperature was changed externally as a parameter. All the experiments were operated under the atmospheric pressure.

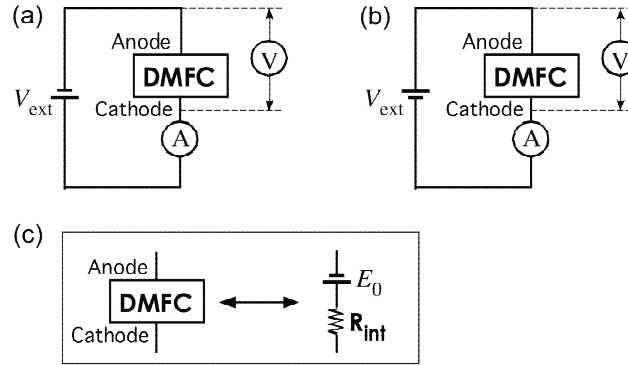


**Fig. 2** Schematic diagrams of the circuits. The external DC power  $V_{\text{ext}}$  is applied in (a): the reverse direction and (b): the forward direction to the cell potential. (c): Equivalent circuit of the DMFC.  $R_{\text{int}}$  and  $E_0$  are internal resistance and open circuit voltage of the cell, respectively.

### 3. Results and Discussion

#### 3.1 Polarization properties

**Figure 3** shows a transient process toward a steady state of the cell potential. The measurement was started immediately after the methanol had been fed into the anode. As seen from the result, the system takes about 20 min to reach a steady state value. In order to skip the transient state the cell was operated for 30 min under an open-circuit condition in advance of each measurement.

Polarization curves were measured with scanning the external resistance to estimate the cell activity. **Figure 4** shows the polarization  $I$ - $V$  curves at the two different temperatures of 35°C and 75°C. The open circuit voltages were approximately 550 mV for 35°C and 620 mV for 75°C. The internal resistances of the cell were almost the same for the two conditions of temperature.

The polarization properties were also measured for the three different methanol concentrations as shown in **Fig. 5**. The cell resistance, which is defined by the slope of the plot, increases with decrease of the concentration.

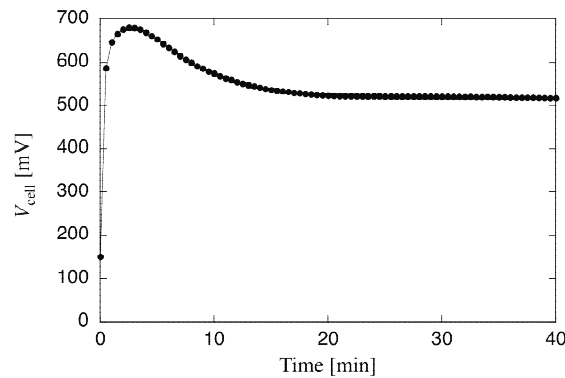


**Fig. 3** Transient process in the cell potential. The voltage was measured under the open circuit condition with 3 wt% methanol.

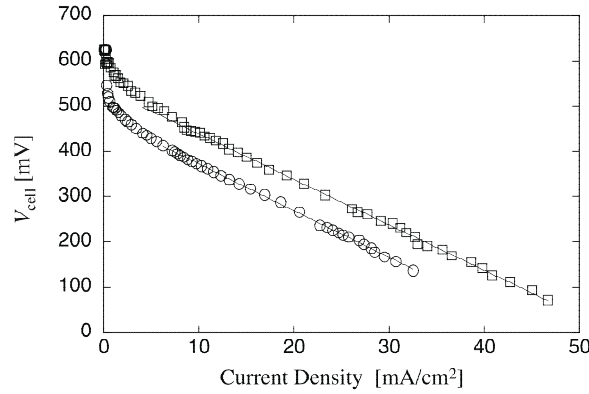


**Fig. 4** Polarization curves measured at the temperatures of 35°C (○) and 75°C (□). Fittings with  $V=E_0-R_{\text{int}}I$  in the linear regime, which are shown by the solid lines, give the values of  $E_0 = 476$  mV for 35°C and  $E_0 = 543$  mV for 75°C.  $R_{\text{int}}$  were approximately  $10 \Omega$  for both temperatures.

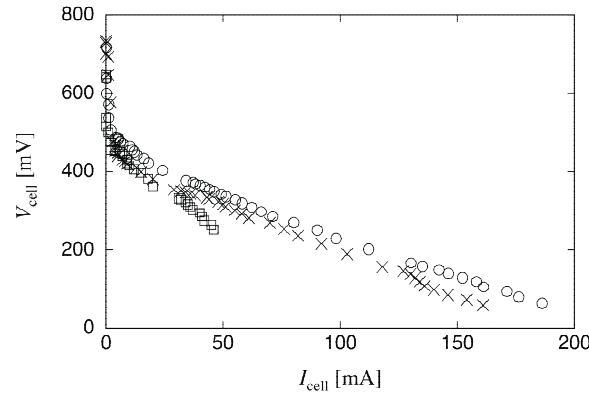


**Fig. 5** Polarization curves for 1 wt% (□), 3 wt% (×) and 5 wt% (○) methanol concentrations.

### 3.2 External potential applied in the reverse direction

The external potential  $V_{\text{ext}}$  was applied in the reverse direction to the cell potential as depicted in **Fig. 2** (a). The  $V_{\text{ext}}$  was increased at a ramp rate of  $V_{\text{ext}} = 0.4$  V/min. The results are shown in **Fig. 6**.

**Figure 6** (a) shows the dependence of the cell potential on  $V_{\text{ext}}$  for the different methanol concentrations. The  $V_{\text{cell}}$  increases linearly with increasing  $V_{\text{ext}}$ , retaining approximately the same value as the  $V_{\text{ext}}$  in the low  $V_{\text{ext}}$  regime regardless of the methanol concentrations. When  $V_{\text{ext}}$  exceeds  $2.5$  V ( $=V^*$ ), on the other hand, the slope of the  $V_{\text{ext}}-V_{\text{cell}}$  plot decreases and the dependence of  $V_{\text{cell}}$  on the methanol concentration appears. The slope is larger for the higher methanol concentration. The results in **Fig. 6** (a) show that there are two stages in the  $V_{\text{ext}}-V_{\text{cell}}$  plot. This trend may reflect that the main reaction process changes in the cell at the threshold value of  $V_{\text{ext}} = V^*$ .

**Figure 6** (b) shows the relation of  $V_{\text{cell}}$  vs.  $I_{\text{cell}}$ . The slope of the  $I_{\text{cell}}-V_{\text{cell}}$  plot gives values of the internal resistance  $R_{\text{cell}}$  of the cell. Consistently with **Fig. 6** (a), dependence of  $R_{\text{cell}}$  on the concentration appears when  $V_{\text{ext}} > V^*$ .

In **Fig. 6** (c) the  $R_{\text{cell}}$  obtained from the slopes in **Fig. 6** (b) were plotted for 2 wt% and 4 wt% of the methanol concentrations.  $R_{\text{cell}}$  has higher values in the low  $V_{\text{ext}}$  regime and becomes small when  $V_{\text{ext}} > V^*$ , for the both concentrations.

**Figure 6** (d) shows the dependence of the  $R_{\text{cell}}$  averaged over the range of  $V_{\text{ext}} > V^*$  on the methanol concentration. The data represent a clear trend that the  $R_{\text{cell}}$  increases with increasing the concentration.

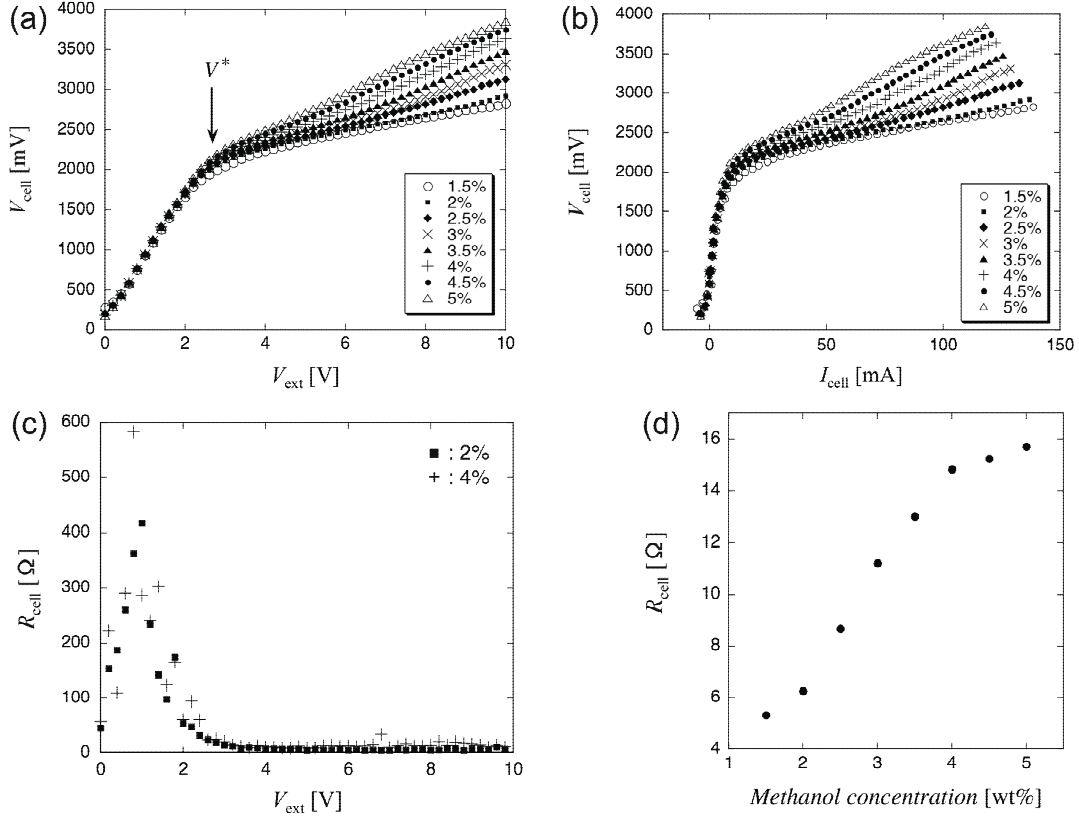


**Fig. 6** The cell potential  $V_{\text{cell}}$  and the cell resistance  $R_{\text{cell}}$  as the responses to the reverse external potential  $V_{\text{ext}}$  for the different methanol concentrations. (a): Dependence of the  $V_{\text{cell}}$  on the  $V_{\text{ext}}$ . (b): Relation of the  $V_{\text{cell}}$  vs. the cell current  $I_{\text{cell}}$ . (c): Dependence of the  $R_{\text{cell}}$  on the  $V_{\text{ext}}$ . (d): The  $R_{\text{cell}}$  averaged over the range of  $V_{\text{ext}} > V^*$  for each methanol concentration.

These results are understood in terms of the following process. Protons and electrons are accumulated by the original cell reactions in the cathode and the anode, respectively. In the low  $V_{\text{ext}}$  regime (below  $V^*$ ) protons and electrons are simply added by the external potential in the cathode and the anode, respectively. Indeed, as seen in the behavior of the  $V_{\text{cell}}$  for the low  $V_{\text{ext}}$  regime, the  $V_{\text{cell}}$  changes in proportion to the  $V_{\text{ext}}$  with the slope of unity, and there is no dependence of the slope on the methanol concentrations. Beyond  $V^*$ , on the other hand,  $V_{\text{ext}}$  becomes high enough to allow the relevant reactions. Thus another chemical reactions start to be promoted by the external potential.

As the reaction proceeds, electrons are fed by the external potential at the anode of the original fuel cell and are consumed on the cathode. When  $V_{\text{ext}}$  becomes relatively high, water electrolysis should take place in the following forms. In the anode side of the fuel cell, the reaction,



proceeds. In the cathode side of the fuel cell, the reaction,



supplies new electrons to the circuit. When the external potential was applied in the reverse direction, small gas bubbles appeared on the electrodes when  $V_{\text{ext}}$  exceeds 1.5 V, indicating that the water electrolysis arises at around  $V_{\text{ext}} = 1.5$  V in the present system. It is considered that the following reactions also supply electrons in the cathode of the fuel cell.



These reactions may occur when  $V_{\text{cell}}$  exceeds 2.0 V including excess polarity in the present experiment as we can infer from **Fig. 6** (a) and (b).

When these reactions promote the electric current in the circuit in the regime above  $V^*$ ,  $R_{\text{cell}}$  and  $V_{\text{cell}}$  become small. Judging from the fact that the  $R_{\text{cell}}$  increases with increasing the methanol concentration in this regime, it is thought that methanol electrolysis also contributes to the changes of the current. When  $V_{\text{cell}}$  is high enough, a sequence of the methanol electrolysis takes place as follows:



The electric decomposition of methanol is induced by the addition of  $\text{H}_2\text{O}$ . Consequently,  $\text{H}_2$  which is generated in each state of the reactions is decomposed by the reaction of  $\text{H}_2 \rightarrow 2\text{H}^+ + 2\text{e}^-$ .

The above interpretation leads to the thought that the high resistance in the low  $V_{\text{ext}}$  regime seen in **Fig. 6** (c) is due to the polarization. When  $V_{\text{ext}}$  exceeds  $V^*$  the electrolysis of water and methanol occur, and the cell resistance becomes small. When the methanol concentration becomes higher, more electrolysis occurs at the anode. The electrolysis generates electrons, and this process prevents the flow of electric current of the original cell reactions. The above consideration agrees with the result seen in **Fig. 6** (d).

### 3.3 External potential applied in the forward direction

The external potential  $V_{\text{ext}}$  was applied in the forward direction to the cell potential as depicted in **Fig. 2** (b). The results are shown in **Fig. 7**.

**Figure 7** (a) shows dependence of the cell potential  $V_{\text{cell}}$  on the  $V_{\text{ext}}$ . The  $V_{\text{cell}}$  decreases as the  $V_{\text{ext}}$  increases. In respect to the change of the slope, the data can be divided into three parts,  $V_{\text{cell}} < V_{\text{ext}}^{*1}$ ,  $V_{\text{ext}}^{*1} < V_{\text{cell}} < V_{\text{ext}}^{*2}$ ,  $V_{\text{ext}}^{*2} < V_{\text{cell}}$  for each concentration as shown by (I), (II) and (III) as seen in **Fig. 7** (a), respectively. When the concentration is higher than 2.5 wt%, the slopes did not change within the range of the experiment. The slopes become larger when  $V_{\text{ext}}$  exceeds  $V_{\text{ext}}^{*1}$  (the region (II)), and become smaller again above  $V_{\text{ext}}^{*2}$  (the region (III)). Different from the reverse external potential case, the dependence of the  $V_{\text{cell}}$  on the methanol concentration is observed in the low  $V_{\text{ext}}$  regime as well.

**Figure 7** (b) shows the relation between  $V_{\text{cell}}$  and cell current  $I_{\text{cell}}$ . The cell resistance  $R_{\text{cell}}$ , which is defined as the slope of the plot, becomes larger as the concentration becomes lower in the low current regime. In the case of the concentration below 2.5 wt%, it is found that the  $V_{\text{ext}}^{*1}$  takes place at lower cell current for the lower methanol concentration. The cell resistances are almost independent of the methanol concentration in the range of  $V_{\text{ext}} > V_{\text{ext}}^{*2}$ .

In **Fig. 7** (c) the  $R_{\text{cell}}$  obtained from the slopes of **Fig. 7** (b) were plotted for 2.5 wt% and 4 wt% of the methanol concentrations. The peak of the  $R_{\text{cell}}$  seen in the data for 2.5 wt% corresponds to the remarkable change of the slope at the intermediate range of the  $V_{\text{ext}}$  observed in **Fig. 7** (b).

**Figure 7** (d) represents the  $R_{\text{cell}}$ , which corresponds to the data in the region (I) of **Fig. 7** (a), with regard to the methanol concentration. The resistance becomes high as the concentration decreases.

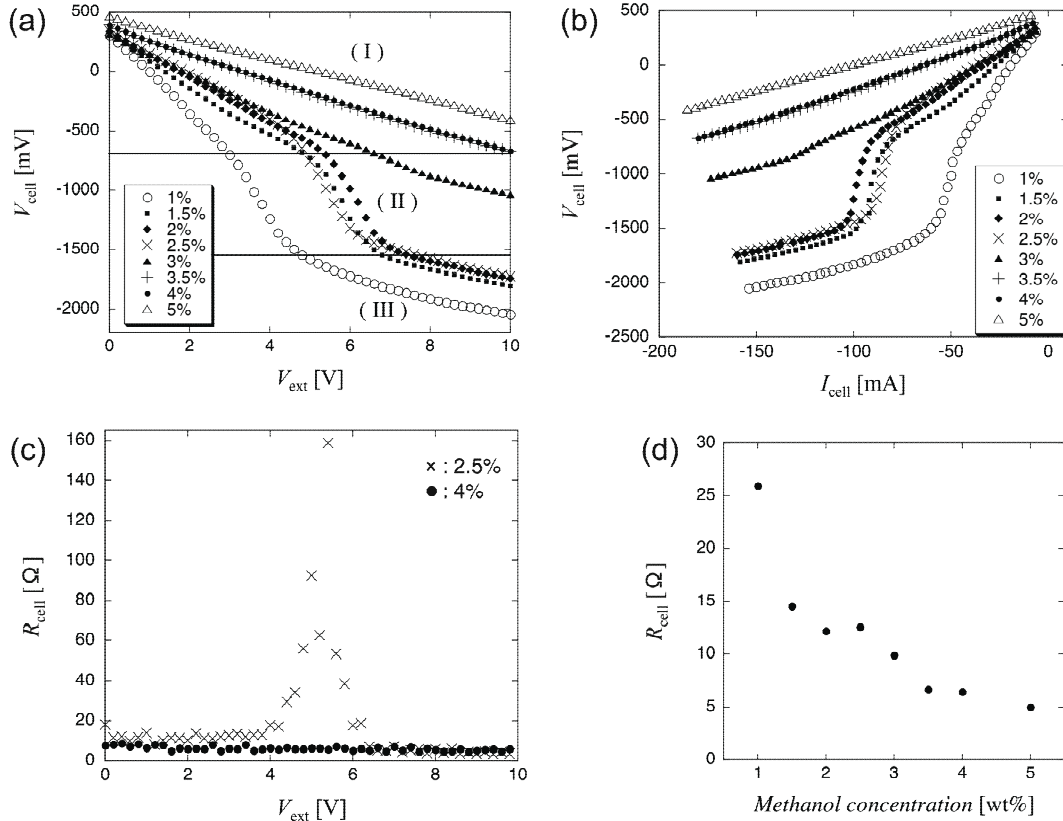


**Fig. 7** The cell potential  $V_{\text{cell}}$  and the cell resistance  $R_{\text{cell}}$  as the responses to the forward external potential  $V_{\text{ext}}$  for the different methanol concentrations. (a): Dependence of the  $V_{\text{cell}}$  on the  $V_{\text{ext}}$ . (b): Relation of the  $V_{\text{cell}}$  vs. the cell current  $I_{\text{cell}}$ . (c): Dependence of the  $R_{\text{cell}}$  on the  $V_{\text{ext}}$ . (d): The  $R_{\text{cell}}$  averaged over the region (I) for each methanol concentration.

These results can be understood by the following process. Protons and electrons are accumulated by the original cell reactions in the cathode and the anode, respectively. Contrary to the reverse external potential case, electrons are taken out from the anode and fed to the cathode when the forward external voltage is applied. Thus the current which is created by the forward external potential reduces the original cell potential. The current depends on the amount of the electrons accumulated by the original cell reactions in the anode, and the amount of the accumulated electrons depends on the methanol concentration. This explains the trend of the cell resistance to the concentration that is seen for the region (I) and concluded in **Fig. 7** (d).

The electrons in the cathode which are accumulated by the external potential react with the protons diffusing towards the cathode. If the density of the protons reaches a steady state and the amount of the diffusing protons is small, the reaction between the protons and electrons does not occur enough fast in the cathode. Then the electrons accumulated in the cathode yield polarization, which makes the cell resistance high. This causes the pronounced change of the resistance, observed for the case of the concentration lower than 2.5 wt%, at the intermediate range of the  $V_{\text{ext}}$  in **Fig. 7** (b). In this situation the internal reaction of the cell changes from the diffusion-limiting process to the reaction-limiting process. It is thought that the cell resistance becomes small beyond  $V_{\text{ext}}^{*2}$  due to the electric decompositions of both water and methanol, which supplies protons and electrons to the circuit.



#### 4. Conclusions

In this study external potentials were applied to the DMFC system in the reverse and the forward direction to the original cell potential in order to investigate the properties of the membrane resistance of the cell. From the dependencies of the resistance on the external potential, it was found that there are thresholds in the external potential at which additional reactions are induced.

When the external potential  $V_{\text{ext}}$  is applied in the reverse direction, two stages of reactions were found in terms of the cell resistance  $R_{\text{cell}}$ , indicating that the main reaction changes in the cell at the threshold,  $V_{\text{ext}}=V^*$ . The cell potential  $V_{\text{cell}}$  increases in proportion with the  $V_{\text{ext}}$  below  $V^*$ . In this regime protons and electrons are simply added in the cathode and the anode, respectively. Above  $V^*$ , on the other hand, additional chemical reactions are promoted by the  $V_{\text{ext}}$ , and  $R_{\text{cell}}$  decreases due to current generated by the reactions. The dependence of the  $R_{\text{cell}}$  on the methanol concentration appears when  $V_{\text{ext}}$  exceeds  $V^*$ , due to the methanol decomposition which is induced at around  $V^*$ .

When the external potential  $V_{\text{ext}}$  is applied in the forward direction, the electrons are drawn from the anode and fed to the cathode by the external potential. Therefore the forward external potential reduces the original cell potential. The cell current depends on the amount of protons and electrons previously accumulated by the original cell reactions and the amount of the accumulated electrons depends on the methanol concentration in the cell. Thus, dependence of  $V_{\text{cell}}$  on the methanol concentration appears even in the low  $V_{\text{ext}}$  region, different from the reverse external potential case. When the density of the protons reaches a steady state, the main reaction occurring at the cell changes from the diffusion-limiting process to the reaction-limiting process. The increase of  $R_{\text{cell}}$  observed for the lower concentrations reflects this reaction resistance. With further increasing the  $V_{\text{ext}}$  the electric decomposition of both water and methanol supplies protons and electrons to the electrodes, and  $R_{\text{cell}}$  becomes independent of the methanol concentration.

#### References

- 1) S. Surampudi, S. R. Narayanan, E. Vamos, H. Frank and G. Halpert, J. Power Sour., Vol.47, pp.377-385 (1994).
- 2) W. Vielstich, J. Braz. Chem. Soc., Vol.14, pp.503-509 (2003).
- 3) A. Hamnett, Catalysis Today, Vol.38, pp.445-457 (1997).
- 4) X. Ren, P. Zelenay, S. Thomas, J. Davey and S. Gottesfeld, J. Power Sour., Vol.86, pp.111-116 (2000).
- 5) V. Gogel, T. Frey, Z. Yongsheng, K. A. Friedrich, L. Jorissen and J. Garche, J. Power Sour., Vol.127, pp.172-180 (2004).
- 6) G. T. Burstein, C. J. Barnett, A. R. Kucernak and K. R. Williams, Catalysis Today, Vol.38, pp.425-437 (1997).
- 7) K. Scott, W. M. Taama, P. Argyropoulos and K. Sundmacher, J. Power Sour. Vol.83, pp.204-216 (1999).
- 8) X. Ren, T. E. Springer and S. Gottesfeld, J. Electrochem. Soc. Vol.147, pp.92-98 (2000).
- 9) G. Q. Lu and C. Y. Wang, J. Power Sour., Vol.134, pp.33-40 (2004).

- 10) M. Shen and K. Scott, J. Power Sour. Vol.148, pp.24-31 (2005).
- 11) P. Argyropoulos, K. Scott and W. M. Taama, J. Power Sour. Vol.87, pp.153-161 (2000).
- 12) C. Xie, J. Bostaph and J. Pavio, J. Power Sour., Vol.136, pp.55-65 (2004).
- 13) H. Wang, J. Hou, H. Yu and S. Sun, J. Power Sour., Vol.165, pp.287-292 (2007).